Progress In Electromagnetics Research M, Vol. 99, 177–189, 2021

Li's Formula Extended to Determine Accurate Resonant Frequency of a Rectangular Patch Antenna in Multi-Dielectric Layers

Manotosh Biswas[1], Sourav Banik[1], and Mihir Dam[2, *]

Abstract—In this article, the drawbacks of Li's formula are rectified and extended to compute accurately the resonant frequency of a rectangular patch antenna in multi-dielectric layers. Computed results employing the present model are compared with experimental and simulation results. The present model shows excellent improvement in accuracy compared to the previously reported investigations.

1. INTRODUCTION

Nowadays microstrip patch antennas (MPA) are very popular, and they are widely used as an efficient sensor [1–3] both on fixed and portable devices [4, 5] due of their several attractive features like light weight, low profile, small size, conformable structure, and easy fabrication. In outdoor application, the antenna performance degrades due to the formation of environmental hazards over the antenna. So, a dielectric cover layer is required to protect the patch from environmental hazards. When a dielectric cover layer is naturally formed or imposed by design, then the effective permittivity of the microstrip structure is changed. Thus, the resonant frequency is shifted. This shift in resonant frequency is used to measure the permittivity of a particular layer in a multi-dielectric layer. So, here the patch antenna behaves like a sensor. Thus the accurate computation of resonant frequency is very essential to use properly the patch antenna as a sensor. Recently, the patch antenna in multi-dielectric superstrate layer draws much attention of the researchers [5–23]. The resonant frequency mainly depends on effective permittivity of the microstrip structure, effective length and width of the patch. So, the accurate computation of these parameters is very crucial. Different theoretical methods have been reported to compute the resonant frequency of the patch in multi-dielectric layers using the variational method [7, 8], multiport network technique [9], and full wave analysis method [10–12]. All of these efforts give reasonably accurate results, but they involve large and rigorous mathematical steps and also take large computational time. The Maxwell or Helmholtz equations for computing the resonant frequency are also very complex and consists of rigorous mathematical steps. So, these techniques are not suitable for computation of the resonant frequency as well as direct synthesis of the patch antenna.

The commercial softwares (HFSS, CST) based on full wave analysis can also be used to compute the resonant frequency. The commercial softwares have also some inherent limitations like they need frequency range and matching impedance location point under the patch for computing the performance properties of the antenna. Without mathematical model, the frequency and matching impedance point are impossible to determine. So, softwares are also not suitable for the direct synthesis of patch antennas. Thus, engineers require a simple closed form model to compute the resonant frequency of a patch antenna loaded with several dielectric layers. The conformal mapping technique is a simple method which is highly suitable to compute the effect of a particular dielectric layer on effective permittivity as well as on

Received 29 August 2020, Accepted 14 November 2020, Scheduled 14 December 2020
* Corresponding author: Mihir Dam (mihir.dam@gmail.com).
[1] Department of Electronics & Tele-Communication Engineering, Jadavpur University, 188, Raja Subodh Chandra Mullick Road, Kolkata, PIN 700 032, India. [2] Department of Electronics, Vidyasagar College for Women, 39 Sankar Ghosh Lane, Kolkata 700 006, India.

resonant frequency of a microstrip patch in multi-dielectric layers. The filling fraction for each dielectric layer is computed by using conformal mapping, and those parameters are used for computation of the effective relative permittivity of the multi-layered structure which ultimately modifies the resonant frequency. The conformal mapping is ideal for design purpose because it consists of fewer mathematical steps and provides closed form expressions. This technique also directly applies to the CAD program and requires less computational time. Thus, conformal mapping technique is employed to investigate the rectangular patch in multi-dielectric structure.

The commercial software HFSS has taken a few minutes time to simulate an antenna (as in Fig. 1), for a usual solver setting (number of passes 50, fast sweep, and frequency step size 0.0005 GHz) in a personal computer having Core i3 processor and 4 GB RAM, whereas the proposed model takes only a fraction of a second to solve the same. So, the proposed model is much faster than simulators and numerical techniques.

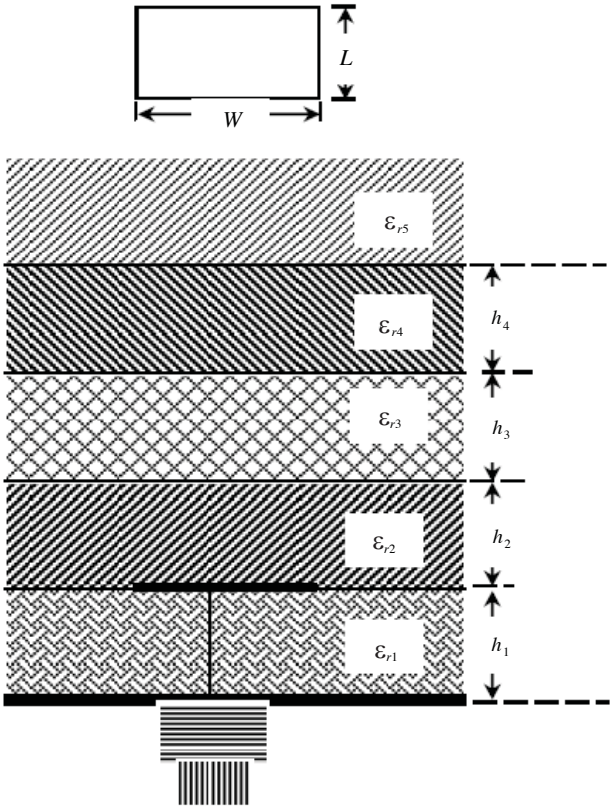

Figure 1. Top view and cross-sectional view of a rectangular patch in multi-dielectric layers.

In order to calculate the resonant frequency of a rectangular patch in multi-dielectric layer, the conformal mapping technique has been employed in [1, 5, 13–17]. Among them [1, 13–16] employed an approximate capacitance formula and erroneous filling fraction arrangements for effective permittivity computation. Also they [13–16] have not incorporated the effect of surface wave and leaky wave in effective length calculation. Later on two efficient conformal mapping approaches were reported in [5, 17]. They [5, 17] used rectified filling fraction arrangements and incorporated the effect of surface wave in effective length calculation. However, these models [5, 17] had some drawbacks: (i) did not consider the effect of leaky wave mode in effective length calculation, (ii) showed higher error for higher permittivity structure, and (iii) valid for only one dielectric cover layer. Very recently, another research group [6] has reported an efficient conformal mapping approach which includes rectified filling fraction arrangements and also incorporates the effect of surface wave. It is also valid for a higher permittivity multilayered structure. However, the model [6] still has some drawbacks: (i) they incorporated the fringing field effect

twice in effective length calculation which is theoretically incorrect; (ii) they did not consider the effect of leaky wave modes in effective length computation; (iii) the previous models [15–21] reported that the resonant frequency of a rectangular patch antenna in multi-dielectric layers decreased with the increase of dielectric cover layer thickness. The article in [22] shows experimentally that the resonant frequency decreases monotonically with the increase of superstrate thickness. The simulation results (HFSS and CST) also support the same nature of previously reported theoretical [15–21] and experimental results [22]. However, the computed resonant frequency using the model [6] shows opposite nature with cover layer thickness which is incorrect. This is based on the fact that the article [6] erroneously calculates the filling fraction of the top layer (air) of the multilayered structure. This is clearly depicted in Fig. 2. The details of the discrepancies are explained in the theory section.

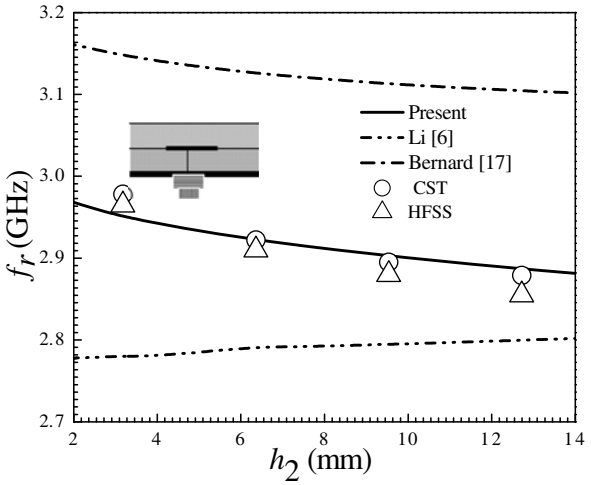

Figure 2. Variation of dominant mode resonant frequency of an ETPA covered with single dielectric layer with the change of dielectric cover thickness h_2. $W = 33.0\,\text{mm}$, $L = 28.0\,\text{mm}$, $h_1 = 3.18\,\text{mm}$, $h_3 = \infty$, $h_4 = 0.0\,\text{mm}$, $\varepsilon_{r1} = \varepsilon_{r2} = 2.32$, $\varepsilon_{r3} = \varepsilon_{r4} = \varepsilon_{r5} = 1.0$.

Considering these inconsistencies of the previous approaches carefully, the development of the present article includes (i) rectification of Li's model and extension to compute the effective permittivity more accurately of the rectangular patch in a multi-dielectric structure, (ii) accurate computation of the effective side length, (iii) inclusion of the effect of leaky wave as well as the surface wave modes in effective length computation, and (iv) validation of the present model with performed experiments, other measurement and simulated values.

2. THEORY

The article [6] reported an expression for computing the resonant frequency for a rectangular patch antenna in multi-dielectric layers (Fig. 1), as

$$f_{r,nml} = \frac{c}{2\left(L_{\mathit{eff}} + 2\Delta L\right)\sqrt{\varepsilon_{r,\mathit{eff}}}} \tag{1}$$

where ΔL is the edge extension due to the fringing fields at the edges of the patch, and it was computed from [23] in the paper [6]. ΔL strongly depends on relative characteristics of substrate and dielectric cover layers. The expression of ΔL reported in [23] is actually for a rectangular geometry without any dielectric cover layer. The authors in [6] used W_{eff} in the place of W and ε_r' in the place of ε_r for incorporating the dielectric cover layer effect in ΔL. The expressions of W_{eff} and ε_r' are obtained from [6] as

$$W_{\mathit{eff}} = \sqrt{\frac{\varepsilon_r'}{\varepsilon_{r,\mathit{eff}}}}\left[\left\{W + 0.882h_1 + 0.164h_1\frac{(\varepsilon_r'-1)}{(\varepsilon_r')^2}\right\} + h_1\frac{(\varepsilon_r'-1)}{\pi\varepsilon_r'}\left\{\ln(0.94 + W/2h_1) + 1.451\right\}\right] \tag{2}$$

$$\varepsilon_r' = \frac{2\varepsilon_{r,eff} - 1 + \left(1 + \dfrac{10h_1}{W_{eff}}\right)^{-1/2}}{1 + \left(1 + \dfrac{10h_1}{W_{eff}}\right)^{-1/2}} \tag{3}$$

The final values of W_{eff} and ε_r' are determined by two-step iteration [17].

L_{eff} is the effective length of the patch. The expression of L_{eff} was reported in [6] as

$$L_{eff} = L\,(1+q)^{\frac{1}{2}} \tag{4}$$

here, q is the fringing field factor which again arises due to the fringing fields at the edges of the patch lengths and was computed from [24]. In [6], they have put $\varepsilon_{re} = \varepsilon_{r1}/\varepsilon_{r,eff}$ to account the effect of substrate and dielectric cover layers. q is also modulated significantly with the relative characteristics of substrate and dielectric cover layers.

Now both ΔL and q arise due to the fringing fields, and both of them have been considered for computing the effective length in [6]. So, Equations (1), (4) [(12) and (13)] of [6] indicate that the article in [6] has incorporated the fringing field effect twice in effective length calculation which is incorrect. To the best of our knowledge, expression (1) was employed first in [6].

Most of the researchers [1, 2, 7–10, 15, 17, 25–36] have used the expression of a rectangular patch with and without dielectric cover layer for computing the resonant frequency instead of Equation (1) as

$$f_{r,nml} = \frac{c}{2\,(L + 2\Delta L)\,\sqrt{\varepsilon_{r,eff}}} \tag{5}$$

Some of the researchers [5, 16, 37–41] have also employed the expression for computing the resonant frequency of rectangular patch with and without dielectric cover layer instead of Equation (1) as

$$f_{r,nml} = \frac{c}{2L_{eff}\,\sqrt{\varepsilon_{r,eff}}} \tag{6}$$

So, either Equation (5) or (6) is correct to compute the resonant frequency of a rectangular patch antenna with and without dielectric cover layer. We have used Equation (5) to compute the resonant frequency.

In this article, we have employed the length extension ΔL due to fringing fields effect as [26]:

$$\Delta L = \frac{\pi r\left(\sqrt{1+q} - 1\right)}{2\,(2.5 - 0.5W/L)} \tag{7}$$

Here, q is the fringing field factor, and it is evaluated from [42, (2), (3)] with $r = L/(\pi - 2)$ [6].

$$q = q_1 + (1+q_1)(q_2 + q_3) \tag{8}$$

$$q_1 = \left(1 + \varepsilon_{re}^{-1}\right)(4h_1/\pi r) \tag{9}$$

$$q_2 = (2/3)\left\{(0.37 + 0.63\varepsilon_{re})^{-1}\,(8 + \pi r/h_1)^{-1}\right\} \times \ln\left[\left\{1 + 0.8\,(r/h_1)^2 + (0.31r/h_1)^4\right\}(1 + 0.9r/h_1)^{-1}\right] \tag{10}$$

$$q_3 = (4 + 2.6r/h_1 + 2.9h_1/r)^{-1}\left\{(0.37 + 0.63\varepsilon_{re})^{-1} - 1\right\} \tag{11}$$

The article reported in [20] has introduced a new relative permittivity ε_{re} of a multilayered structure for accounting the effect of surface wave due to surface wave mode. ε_{re} is used to compute the fringing field factor q. The ε_{re} for multi-layered structure was defined in [20] as

$$\varepsilon_{re} = \frac{\varepsilon_{r1}}{\varepsilon_{r,eff}} \tag{12}$$

The derivation for computing ε_{re} was not reported in [20], and only the expression was provided [20, Equation (11)]. Here we have accounted the effect of leaky wave mode in a similar manner of surface wave mode [20]. The leaky wave is accounted in terms of fringing field. This fringing field very much

depends on the relative characteristics of the substrate and dielectric cover layer. Recently, the effect of leaky wave mode on microstrip structure draws much attention of the researchers [43–46]. These studies show that the leaky wave due to leaky wave mode has significant impact on antenna performances. The leaky wave due to leaky wave mode very much depends on the relative characteristics of substrate and dielectric cover layers as indicated by [45, 46]. They [45, 46] showed that leaky wave due to leaky wave mode will be reduced very much when the relative permittivity of the dielectric cover layer is larger than that of the substrate for a particular substrate and dielectric cover layer thickness combination. We have accounted the effect of both surface wave and leaky wave in effective patch length computation for further improvement in results. Based on these two facts (surface wave and leaky wave modes), we have proposed a new relative permittivity to compute the fringing field as

$$\varepsilon_{re} = \frac{\varepsilon_r'}{\varepsilon_{r,eff}} \tag{13}$$

With this new relative permittivity more improvement in results is obtained. ε_r' is defined in Equation (3). We have put the value of ε_{re} from Equation (13) instead of Equation (12) for computing fringing filed factor q [in Equations (9)–(11)]. All the models reported in [1, 5, 6, 7, 13–17] did not consider the effect of leaky waves in effective length calculation. The justification of Equation (13) is verified in result section in Table 4. From the above discussion it is understood that we have incorporated the fringing field effect once in effective length computation.

For computing the effective permittivity, Svacina employed conformal mapping technique for generalized multilayered microstrip [14]. Here, the patch is placed on single substrate and covered by four dielectric superstrate layers (top layer is air) as depicted in Fig. 1. Now, the structure is mapped onto a complex g-plane ($g = u + iv$) in Fig. 3 using conformal mapping techniques as described by Svacina [14]. The ratio of each dielectric area A_i ($i = 1, 2, \ldots, 5$) to the total area of the cross section A_{tot} in the g-plane is defined as filling fraction for each layer. The filling fractions ($p_i = A_i/A_{tot}$) for these five layers are expressed as

$$p_1 = \frac{A_1}{A_{tot}} = 1 - \frac{h_1}{2W_{eff}} \ln\left(\frac{\pi}{h_1} W_{eff} - 1\right) \tag{14}$$

$$p_i = \frac{A_i}{A_{tot}} = \frac{h_1}{2W_{eff}} \left\{ \ln\left(\frac{\pi}{h_1} W_{eff} - 1\right) - (1 + g_i) \times \ln\left[\frac{2W_{eff}}{h_1} \frac{\cos\left(\frac{\pi}{2} g_i\right)}{\frac{2h_i}{h_1} - 1 + g_i} + \sin\left(\frac{\pi}{2} g_i\right)\right] \right\} \tag{15}$$

$$i = 2, 3, 4$$

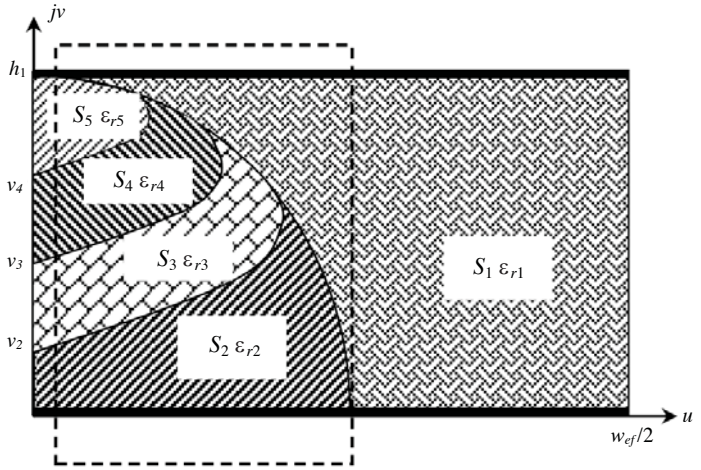

Figure 3. Equivalent parallel plate arrangement using conformal mapping.

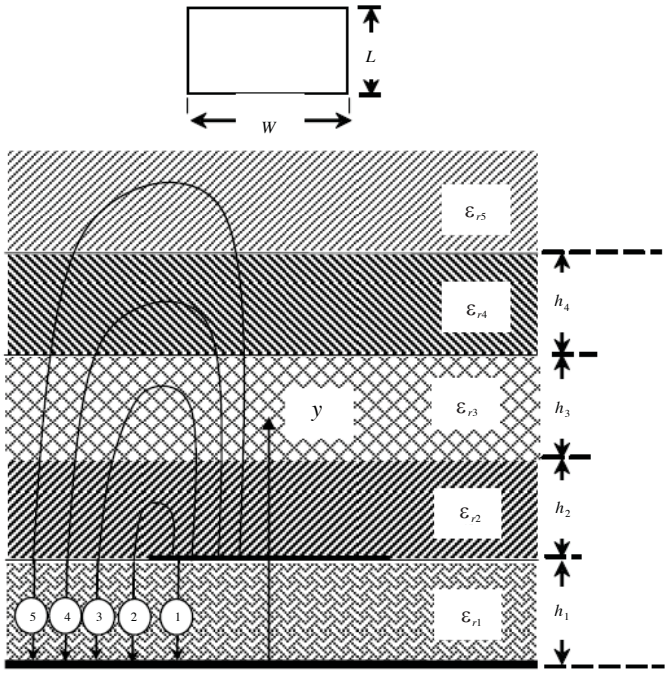

Figure 4. Electric flux in different paths for the structure depicted in Fig. 1.

$$g_i = \frac{2}{\pi}\arctan\left[\frac{\pi}{\frac{\pi}{2}\frac{W_{eff}}{h_1} - 2}\left(\frac{h_i}{h_1}\right) - 1\right] \tag{16}$$

where W_{eff} is computed from Equation (2).

$$p_5 = 1 - \sum_{j=2}^{4} p_j - p_1 \quad i = 2, 3, 4 \tag{17}$$

Now, the important situation is that when any of the top superstrate layers is absent, the filling fraction of the corresponding layer should be zero. However, in this situation the filling fraction of the top superstrate layers computed from Equation (15) provides a non-zero value. It means that the value of top layers filling fractions is overestimated. To correct this discrepancy, filling fractions are required to recalibrate. Now, to correct these filling fractions we require to study the paths of the electric field flux lines from patch to ground plane (Fig. 4). From Fig. 4, it is observed that the electric field flux lines from patch can propagate through five different paths to reach the ground plane. In path 1, the flux remains within the substrate. For paths 2 to 4, the flux lines propagate in substrate and top superstrate layers with different relative permittivities, and in path 5, the flux lines pull out to the space. The arrangements of the new filling fractions based on these electric field flux lines from patch to ground plane are depicted in Fig. 5. Now, the recalibrated filling fractions may be expressed as [6]:

$$p_{11} = p_1 - 2p_{20} - p_{40} \tag{18}$$

$$p_{ii} = [1 - p_{11} - p_5 - 2p_{20} - p_{30} - p_{40}] \times (p_i - p_{i0}) \left[\sum_{j=2}^{4} p_j - p_{j0}\right]^{-1} \tag{19}$$

$$i = 2, 3, 4$$

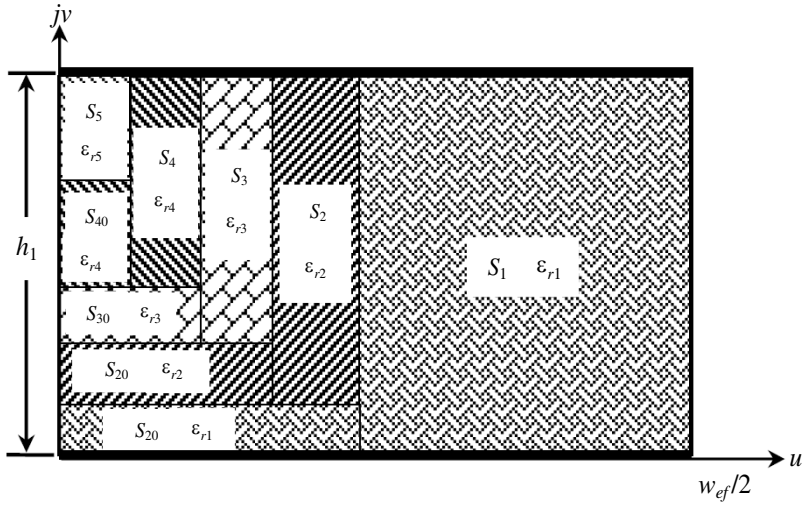

Figure 5. Filling fraction arrangement following the electric flux paths depicted in Fig. 4 for effective permittivity computation.

$$p_{i0} = \frac{h_1}{2W_{eff}} \left\{ \ln\left(\frac{\pi}{h_1}W_{eff} - 1\right) - (1+g_{i-1}) \times \ln\left[\frac{2W_{eff}}{h_1}\frac{\cos\left(\frac{\pi}{2}g_{i-1}\right)}{\frac{2h_{i-1}}{h_1} - 1 + g_{i-1}} + \sin\left(\frac{\pi}{2}g_{i-1}\right)\right]\right\} \quad (20)$$
$$i = 2,3,4$$

Now, the article in [6] has taken the filling fraction for the top layer (air) p_5 instead of p_{55} for the computation of $\varepsilon_{r,eff}$, which shows the variation of resonant frequency with dielectric cover layer thickness opposite in nature. The validation of this statement is verified in Fig. 2. p_5 is the initial approximate filling fraction of top layer (air). Here, we propose the rectified filling fraction p_{55} for the top layer as

$$p_{55} = 1 - \sum_{j=2}^{4} p_{jj} - p_{11} \quad (21)$$

With this rectified filling fraction, we have computed correct value of $\varepsilon_{r,eff}$ which shows that the computed resonant frequency decreases with the increase of dielectric cover layer thickness (Fig. 2).

Considering these recalibrated filling fractions, the effective permittivity of this structure (as in Fig. 5) can be computed as [6]:

$$\begin{aligned} \varepsilon_{r,eff} &= \varepsilon_{r1}p_{11} + \varepsilon_{r1}u\left(p_{22}+p_{33}+p_{44}+p_{55}+4p_{20}\right)^2 \\ &\quad \times \left[\varepsilon_{r1}\left(p_{22}+p_{33}+p_{44}+p_{55}+3p_{20}\right)^2 + up_{20}\right]^{-1} \quad (22) \\ u &= \varepsilon_{r2}p_{22} + \varepsilon_{r2}\left(\varepsilon_{r3}p_{33}+v\right)\left(p_{33}+p_{44}+p_{55}+3p_{20}\right)^2 \\ &\quad \times \left[\varepsilon_{r2}\left(p_{33}+p_{44}+p_{55}+2p_{20}\right)^2 + \left(\varepsilon_{r3}p_{33}+v\right)p_{20}\right]^{-1} \quad (23) \end{aligned}$$

and

$$\begin{aligned} v &= \varepsilon_{r3}\left[\varepsilon_{r4}p_{44} + \varepsilon_{r4}\varepsilon_{r5}\left(p_{55}+p_{20}\right)^2 \times \left(\varepsilon_{r4}p_{55}+\varepsilon_{r5}p_{20}\right)^{-1}\right] \\ &\quad \times \left(p_{44}+p_{55}+2p_{20}\right)^2 \times \left\{\varepsilon_{r3}\left(p_{44}+p_{55}+p_{20}\right)^2 + p_{20}\right. \\ &\quad \left. \times \left[\varepsilon_{r4}p_{44} + \varepsilon_{r4}\varepsilon_{r5}\left(p_{55}+p_{20}\right)^2 \times \left(\varepsilon_{r4}p_{55}+\varepsilon_{r5}p_{20}\right)^{-1}\right]\right\} \quad (24) \end{aligned}$$

3. ANTENNA DESIGN AND EXPERIMENTAL TESTS

A prototype has been etched on Taconic dielectric substrates ($\varepsilon_{r1} = 2.33$, $h_1 = 0.7875\,\text{mm}$). The patch is excited with a coaxial probe whose diameter $g = 1.24\,\text{mm}$. Different dielectric substrates like Taconic, Rogers, Glass epoxy, Arlon, etc. with different thicknesses and relative permittivities used as dielectric cover layers. To validate the model developed in Section 2, we perform a set of experiments using Network Analyzer Agilent-E5071B. It is very easy to find the resonant frequency of an antenna using network analyzer. During the testing of an antenna with network analyzer, the resonant frequency can be measured from — (i) impedance locus in Smith chart (at zero reactance value) or (ii) s_{11} variation (minimum value of s_{11} point). Here we follow the second approach to find resonant frequency.

4. RESULTS AND DISCUSSIONS

Today several articles have been published in different renowned journals using the results based on simulation tools (HFSS, IE3D, CFDTD, CST, etc.) because simulation provides quite accurate results within a short time very easily. In this article, most of the HFSS simulated values of Rectangular Patch Antenna in Multi-dielectric Layers (Tables 2, 3, 4) are taken from the article [6]. We have also employed HFSS in Table 1 in this paper comfortably for a usual solver setting (number of passes 50, fast sweep and frequency step size 0.0005 GHz) in a personal computer having Core i3 processor and 4 GB RAM which gives the results within a few minutes.

Table 1. Comparison of theoretical, HFSS simulation and experimental resonant frequencies for a rectangular patch sensor covered with three layered dielectric superstrates. $W = 30.0\,\text{mm}$, $L = 24.0\,\text{mm}$, $h_1 = 0.7875\,\text{mm}$, $h_2 = h_4 = 0.8265\,\text{mm}$, $\varepsilon_{r1} = 2.33$, $\varepsilon_{r2} = \varepsilon_{r4} = 2.4$, $\varepsilon_{r5} = 1.0$.

ε_{r3}	h_3 (mm)	Resonant frequency (GHz)				
		Exp.	HFSS	Computed		
				Present	Li[1]	Li[2]
2.2	0.508	3.799	3.791	3.748	3.975	3.896
2.33	0.7875	3.792	3.785	3.746	3.974	3.894
2.33	1.575	3.753	3.780	3.743	3.987	3.909
2.33	1.58	3.739	3.778	3.743	3.987	3.909
2.55	2.34	3.729	3.736	3.736	3.979	3.900
5.0	1.63	3.695	3.720	3.696	3.950	3.868
5.6	1.4	3.689	3.710	3.692	3.941	3.858
10.0	1.63	3.611	3.615	3.620	3.909	3.823
Average % Error with respect to Exp				**0.434**	**6.374**	**4.208**
Average % Error with respect to HFSS				**0.667**	**5.988**	**3.830**

Li[1]: Used corrected Equation (5) for f_r calculation [6].
Li[2]: Used corrected Equation (6) for f_r calculation [6].

It has already been mentioned in theory section that the expression employed in [6] for calculating the effective length was erroneous. So, for the model in [6], we have taken correct expressions (5) and (6) in the entire experimental tables.

4.1. Sensor Covered with Three Dielectric Layered Structures

In Table 1, we compare our experimental and simulated (HFSS) resonant frequencies with theoretical values for a rectangular patch sensor covered with a three layered dielectric superstrate. Now from this comparison it is clear that the computed resonant frequencies employing the present model are more accurate and far better than [6].

Table 2. Comparison of theoretical, HFSS simulation and experimental resonant frequencies for a rectangular patch sensor covered with three layered dielectric superstrates. $W = 10.0\,\text{mm}$, $L = 10.0\,\text{mm}$, $h_1 = 0.98\,\text{mm}$, $h_2 = h_4 = 0.508\,\text{mm}$, $\varepsilon_{r1} = 1.046$, $\varepsilon_{r2} = \varepsilon_{r4} = 3.27$, $\varepsilon_{r5} = 1.0$.

ε_{r3}	h_3 (mm)	Resonant frequency (GHz)				
		Exp. [6]	HFSS	Computed		
				Present	Li[1]	Li[2]
1	1.100	11.150	10.975	10.737	12.199	12.224
1.046	1.100	11.175	10.975	10.718	12.180	12.197
1.067	10.200	11.350	11.150	10.878	12.415	12.526
1.093	10.200	11.325	11.125	10.850	12.390	12.491
2.1	1.000	10.700	10.525	10.374	11.776	11.639
3.00	0.508	10.575	10.375	10.270	11.595	11.390
4.5	0.508	10.350	10.175	10.051	11.398	11.125
6.00	0.635	9.950	9.850	9.755	11.159	10.804
6.15	0.635	9.900	9.775	9.734	11.144	10.785
9.20	0.635	9.475	9.425	9.333	10.906	10.468
9.8	0.635	9.475	9.375	9.261	10.868	10.419
10.2	0.635	9.400	9.325	9.214	10.845	10.387
Average % Error with respect to Exp				**2.862**	**11.409**	**9.322**
Average % Error with respect to HFSS				**1.488**	**12.979**	**10.871**

Li[1]: Used corrected Equation (5) for f_r calculation [6].
Li[2]: Used corrected Equation (6) for f_r calculation [6].

The validity of the present model for a rectangular patch sensor covered with a three-layered dielectric superstrate is further validated in Table 2. Here the computed values employing the present model and model reported in [6] are compared with the measurement in [6]. The computed resonant frequencies employing the present model show excellent agreement with simulated and experimental results compared to the model in [6].

4.2. Sensor Covered with Two Dielectric Layered Structures

In Table 3, we compare simulated and measured [6] resonant frequencies with theoretical values for a rectangular patch sensor covered with a two-layered dielectric superstrate. It is observed that the computed resonant frequencies employing the present model are in close correlation with simulation and measured [6] results compared to the model in [6].

4.3. Sensor Covered with Single Dielectric Layered Structures

In Table 4, different theoretical values of resonant frequency employing the present model and model reported in [6, 17] for a rectangular patch sensor covered with single layered dielectric superstrate are compared with measurement [6] and simulation (HFSS) values. The comparison shows that computed resonant frequencies employing present model show very close agreement with simulated and experimental results compared to others [6, 17].

More accurate results are obtained with the present model due to consideration of the proper filling fraction arrangement for top layer, correct effective patch length computation, and minimized effect of leaky wave as well as surface wave.

Table 3. Comparison of theoretical, HFSS simulation and experimental resonant frequencies a rectangular patch sensor covered with two layered dielectric superstrates. $W = 10\,\text{mm}$, $L = 10\,\text{mm}$, $h_1 = 0.99\,\text{mm}$, $h_4 = 0.00\,\text{mm}$, $\varepsilon_{r1} = 1.046$, $\varepsilon_{r3} = \varepsilon_{r4} = \varepsilon_{r5} = 1.0$.

ε_{r2}	h_2 (mm)	ε_{r3}	h_3 (mm)	Resonant frequency (GHz)				
				Exp. [6]	HFSS	Computed		
						Present	Li[1]	Li[2]
3.27	0.508	6.00	0.635	9.975	10.070	9.842	11.237	10.912
		9.20	0.635	9.450	9.625	9.352	10.962	10.546
6.00	0.635	3.27	0.508	9.700	9.675	9.553	10.583	10.583
		9.20	0.635	8.900	8.825	8.757	9.409	9.409
9.20	0.635	3.27	0.508	9.000	8.950	8.821	9.934	9.934
		6.00	0.635	8.600	8.550	8.495	10.884	9.351
Average % Error with respect to Exp						**1.450**	**13.402**	**9.154**
Average % Error with respect to HFSS						**1.536**	**13.296**	**9.049**

Li[1]: Used corrected Equation (5) for f_r calculation [6].
Li[2]: Used corrected Equation (6) for f_r calculation [6].

Table 4. Comparison of theoretical, HFSS simulation and experimental resonant frequencies a rectangular patch sensor covered with single dielectric superstrates. $W = 10.0\,\text{mm}$, $L = 10.0\,\text{mm}$, $h_1 = 0.98\,\text{mm}$, $h_3 = \infty$, $h_4 = 0.0\,\text{mm}$, $\varepsilon_{r1} = 1.046$, $\varepsilon_{r3} = \varepsilon_{r4} = \varepsilon_{r5} = 1.0$.

ε_{r2}	h_2 (mm)	Resonant frequency (GHz)						
		Exp. [6]	HFSS	Computed				
				Present		Li[1]	Li[2]	Ber[1] [17]
				$\varepsilon_{re} = \varepsilon'_r/\varepsilon_{reff}$	$\varepsilon_{re} = \varepsilon_{r1}/\varepsilon_{reff}$			
3.00	0.508	11.325	11.325	11.136	10.927	12.761	13.019	12.173
3.27	0.508	11.200	11.175	11.064	10.84	12.697	12.927	12.134
4.50	0.635	10.950	10.750	10.617	10.302	12.335	12.414	11.972
6.00	0.635	10.300	10.025	10.219	9.8258	12.014	11.966	11.706
6.15	0.635	10.100	10.025	10.181	9.7805	11.984	11.925	11.688
9.20	0.635	9.525	9.250	9.474	8.9432	11.459	11.207	11.361
9.80	0.635	9.475	9.150	9.349	8.7953	11.370	11.088	11.305
10.2	0.635	9.075	9.075	9.267	8.6994	11.314	11.012	11.268
Average % Error with respect to Exp				**1.437**	**4.729**	**17.370**	**16.751**	**14.661**
Average % Error with respect to HFSS				**1.763**	**3.205**	**19.154**	**18.512**	**16.417**

Li[1]: Used corrected Equation (5) for f_r calculation [6].
Li[2]: Used corrected Equation (6) for f_r calculation [6].
Ber[1]: [17].

5. CONCLUSION

In this article, a very simple and accurate model is presented to determine the resonant frequency of a rectangular patch antenna in multi-dielectric layers. This work is an extension of Li's work. The drawback of the prior work for computing the top layer filling fraction has been corrected for accurate computation of the effective permittivity. We have corrected the erroneous effective patch length expression of previous work. We have also minimized the effect of leaky wave in addition to surface wave for more tuning in results which is not reported earlier. The correction of Li's model as well as the consideration of leaky wave reduces error of the model with respect to the experimental and simulated results. Here the accuracy means accuracy with respect to simulation and experiments. This model is very efficient and capable of very accurately predicting the resonant frequency for wide range variation of substrate and dielectric cover layers parameters.

REFERENCES

1. Bogosanovich, M., "Microstrip patch sensor for measurement of the permittivity of homogeneous dielectric materials," *IEEE Trans. Instrum. Meas.*, Vol. 49, 1144–1148, 2000.
2. Verma, A. K., Nasimuddin, and A. S. Omar, "Microstrip resonator sensors for determination of complex permittivity of materials in sheet, liquid and paste forms," *Proc. Ins. Elect. Eng.*, Vol. 152, 47–54, 2005.
3. Zucchelli, A., M. Chimenti, E. Bozzi, and P. Nepa, "Application of a coaxial-fed patch to microwave non-destructive porosity measurements in low-loss dielectrics," *Progress In Electromagnetics Research M*, Vol. 5, 1–14, 2008.
4. Biswas, M. and M. Dam, "CAD oriented improved cavity model to investigate a 30°-60°-90° right angled triangular patch antenna on single, composite and suspended substrate for the application in portable wireless equipments," *IET Microw. Antennas Propagat.*, Vol. 12, No. 3, 425–434, 2018.
5. Biswas, M. and M. Sen, "Design and development of rectangular patch antenna with superstrates for the application in portable wireless equipments and aircraft radome," *Microw. Opt. Tech. Lett.*, Vol. 56, 883–893, 2014.
6. Li, Y. and N. Bowler, "Resonant frequency of a rectangular patch sensor covered with multilayered dielectric structures," *IEEE Trans. Antennas Propagat.*, Vol. 58, 1883–1889, 2010.
7. Bahl, J., P. Bhartia, and S. Stuchly, "Design of microstrip antennas covered with a dielectric layer," *IEEE Trans. Antennas Propagat.*, Vol. 30, 314–318, 1982.
8. Verma, A. K., "Analysis of rectangular patch antenna with dielectric cover," *IEICE Trans.*, Vol. 74, 1270–1275, 1991.
9. Benalla, A. and K. C. Gupta, "Multiport network model for rectangular microstrip patches covered with a dielectric layer," *IEE Proc.*, Vol. 137, 377–383, 1990.
10. Qasim, G. and S. Zhong, "Resonant frequency of a rectangular microstrip antenna covered with dielectric layer," *J. Shanghai Univ. of Sci. & Tech.*, Vol. 14, 77–84, 1991.
11. Nelson, R. M., D. A. Rogers, and A. G. D'Assuncio, "Resonant frequency of a rectangular microstrip patch on several uniaxial substrates," *IEEE Trans. Antennas Propagat.*, Vol. 38, 978–981, 1990.
12. Pribetich, J., "Modelling of microstrip antenna with dielectric protective layer for lossy medium," *Electron Lett.*, Vol. 24, 1464–1465, 1988.
13. Svacina, J., "Analysis of multilayer microstrip lines by a conformal mapping method," *IEEE Trans. Microw. Theory Tech.*, Vol. 40, 769–772, 1992.
14. Svacina, J., "A simple quasi-static determination of basic parameters of multilayer microstrip and coplanar waveguide," *IEEE Microw. Guided Wave Lett.*, Vol. 2, 385–387, 1992.
15. Zhong, S.-S., G. Liu, and G. Qasim, "Closed form expressions for resonant frequency of rectangular patch antennas with multidielectric layers," *IEEE Trans. Antennas and Propagat.*, Vol. 42, 1360–1363, 1994.
16. Biswas, M., S. Banik, M. Biswas, and A. Sukla, "CAD model to predict the effect of radome on the characteristics of rectangular patch antenna," *Microw. Opt. Tech. Lett.*, Vol. 55, 2460–2468, 2013.

17. Bernhard, J. T. and C. J. Tousignant, "Resonant frequencies of rectangular microstrip antennas with flush and spaced dielectric superstrates," *IEEE Trans. Antennas Propagat.*, Vol. 47, 302–308, 1999.
18. Biswas, M. and A. Mandal, "Experimental and theoretical investigation of resonance and radiation characteristics of superstrate loaded rectangular patch antenna," *Microw. Opt. Tech. Lett.*, Vol. 57, 791–799, 2014.
19. Biswas, M. and D. Guha, "Input impedance and resonance characteristic of superstrate loaded triangular microstrip patch," *IET Microw. Antennas Propagat.*, Vol. 3, 92–98, Feb. 2009.
20. Guha, D. and J. Y. Siddiqui, "Resonant frequency of circular microstrip antenna covered with dielectric superstrate," *IEEE Trans. Antennas Propagat.* Vol. 51, 1649–1652, 2003.
21. Losada, V., R. R. Boix, and M. Horno, "Resonant modes of circular microstrip patches in multilayered substrates," *IEEE Trans. Microw. Theory Tech.*, Vol. 47, 488–497, 1999.
22. Bhattacharyya, A. and T. Tralman, "Effects of dielectric superstrate on patch antennas," *Electron. Lett.*, Vol. 24, 356–358, Mar. 1988.
23. Kirschning, M., R. H. Jansen, and N. H. L. Koster, "Accurate model for open end effect of microstrip lines," *Electron. Lett.*, Vol. 17, 123–125, Feb. 1981.
24. Guha, D., "Resonant frequency of circular microstrip antennas with and without air gaps," *IEEE Trans. Antennas Propagat.*, Vol. 49, 55–59, Jan. 2001.
25. Garg, R., P. Bhartia, I. Bahl, and A. Ittipiboon, *Microstrip Antenna Design Handbook*, Artech House, Canton, MA, 2001.
26. Chattopadhyay, S., B. Biswas, J. Y. Siddiqui, and D. Guha, "Rectangular microstrips with variable air gap and varying aspect ratio: Improved formulations and experiments," *Microw Opt. Tech. Lett.*, Vol. 51, 169–173, 2009.
27. James, J. R. and P. S. Hall, *The Handbook of Microstrip Antennas*, Vol. 1 & 2, Peter Peregrinus Ltd., London, 1989.
28. Chattopadhyay, S., M. Biswas, J. Y. Siddiqui, and D. Guha, "Input impedance of probe-fed rectangular microstrip antennas with variable air gap and varying aspect ratio," *IET Microw. Antennas Propagat.*, Vol. 3, 1151–1156, 2009.
29. Ali, A., "A closed-form expression for the resonant frequency of rectangular microstrip antennas," *Microw. Opt. Tech. Lett.*, Vol. 49, No. 8, 1848–1852, 2007.
30. Kara, M., "Closed-form expressions for the resonant frequency of rectangular microstrip antenna elements with thick substrates," *Microw. Opt. Technol. Lett.*, Vol. 12, No. 3, 131–136, 1996.
31. Verma, A. K. and Z. Rostamy, "Modified Wolff model for determination of resonance frequency of dielectric covered circular microstrip patch antenna," *Electron. Lett.*, Vol. 27, No. 24, 2234–2236, 1991.
32. Verma, A. K., "Resonant frequency of uncovered and covered rectangular microstrip patch using modified Wolff model," *IEEE Trans. Microw. Theory Tech.*, Vol. 41, No. 1, 109–116, 1993.
33. Guney, K., "A new edge extention expression for the resonant frequency of rectangular microstrip antennas with thin and thick substrates," *J. Commun. Tech. Electron.* Vol. 49, 49–53, 2004.
34. Sengupta, D. L., "Approximate expression for the resonant frequency of rectangular patch antenna," *Electron. Lett.*, Vol. 19, 834–835, 1983.
35. Lo, Y. T., D. Solomon, and W. F. Richards, "Theory and experiment on microstrip antennas," *IEEE Trans. Antennas Propagat.*, Vol. 27, 137–145, 1979.
36. Chew, W. C. and Q. Liu, "Resonance frequency of a rectangular microstrip patch," *IEEE Trans. Antennas Propagat.*, Vol. 36, 1045–1056, 1988.
37. Carver, K. R. and E. L. Coffey, *Theoretical Investigation of the Microstrip Antenna*, 1979.
38. Biswas, M. and A. Mandal, "Experimental and theoretical investigation of resonance and radiation characteristics of superstrate loaded rectangular patch antenna," *Microw. Opt. Tech. Lett.*, Vol. 57, 791–799, 2014.
39. Biswas, M. and A. Mandal, "Experimental and theoretical investigation to predict the effect of superstrate on the impedance, bandwidth, and gain characteristics for a rectangular patch antenna,"

Journal of Electromagnetic Waves and Applications, Vol. 29, No. 16, 2093–2109, 2015.

40. Abboud, F., J. P. Damiano, and A. Papiernik, "Simple model for the input impedance of coax-fed rectangular microstrip patch antenna for CAD," *IEE Proc. Pt. H.*, Vol. 1, No. 35, 323–326, 1988.
41. Long, S. A. and R. Garg, "Resonant frequency of electrically thick rectangular microstrip antenna," *Electron. Lett.*, Vol. 23, No. 21, 1149–1151, 1987.
42. Biswas, M. and S. Banik, "Characteristics of circular patch antenna with and without air gaps," *Microw. Opt. Tech. Lett.*, Vol. 54, 1692–1699, 2012.
43. Mesa, F., D. R. Jackson, and M. J. Freire, "Evolution of leaky modes on printed-circuit lines," *IEEE Trans Microw. Theory Tech.*, Vol. 50, 94–104, 2002.
44. Nghiem, D., J. T. Williams, D. R. Jackson, and A. A. Oliner, "Existence of a leaky dominant mode on microstrip line with an isotropic substrate: Theory and measurements," *IEEE Trans. Microwave Theory Tech.*, Vol. 44, 1710–1715, 1996.
45. Peixeiro, C. and A. M. Barbosa, "Leaky and surface waves in anisotropic printed antenna structures," *IEEE Trans. Antennas Propagat.*, Vol. 40, 566–569, 1992.
46. Jackson, D. R. and A. A. Oliner, "A leaky-wave analysis of the high-gain printed antenna configuration," *IEEE Trans. Antennas Propagat.*, Vol. 36, 905–910, 1988.